JOURNAL OF MATERIALS SCIENCE 16 (1981) 2091–2102

A second-order erosion slowness theory of the development of surface topography by ion-induced sputtering

G. CARTER, M. J. NOBES, R. P. WEBB
Department of Electrical Engineering, University of Salford, Salford, UK

The spatial variation of energy deposited in a solid can lead to local variations in sputtering yield at points on the surface neighbouring the point of ion impact. An approximate theory is developed to describe this local sputtering yield variation in terms of the local morphology. It is then shown how, if this local variation merely moderates the standard sputtering yield–projectile incidence angle function by multiplication, an erosion slowness theory can be simply modified and generalized to allow prediction of the time development of sputtered surface morphology. Both transient and steady-state morphologies are explored.

1. Introduction

The development of surface topography during ion-induced sputtering of solids is becoming relatively well documented experimentally [1, 2] and a number of theories have been developed to model the observations within random, amorphous solids [3–5] or crystalline solids [6, 7]. A characteristic feature of such theories is that, with one exception [8], they associate primary changes in morphology only with the variations of local surface erosion rate with ion flux incidence angle to the local surface. Other secondary processes occurring either concomitantly with and/or as a result of ion irradiation have been discussed and these include surface and volume atomic migration and diffusion [9, 10], sputtered atom redeposition [11–15] and locally variable incident ion flux arising from particle reflection from neighbouring surface elements [11–15]. The role of perturbations in local erosion rate resulting from (a) native contaminants, impurities, inclusions and imperfections [1, 2], (b) radiation-induced imperfactions [6, 7], and (c) spatial variations in ion flux density [16–19], has also been discussed in detail.

Only in the work of Sigmund [8], however, has any attention been devoted to the influence of the microscopic details of the sputtering phenomenon on macroscopic erosion processes. Thus Sigmund [8] considered the surface spatial distribution of atomic sputtering ejection relative to the position of ion impingement on a surface resulting from the volume spatial distribution of the energy deposition from the projectile and atomic recoils in a linear cascade model and the intersection of this energy deposition profile with the surface. By considering the differences in local energy deposition on infinite plane surfaces and at conjunctions of differently orientated semi-infinite planes, Sigmund [8] concluded that the erosion rates of corners or edges would be different from the erosion rates of the bounding planes and would be relatively enhanced or reduced according to whether the bounding planes and conjunction formed included or excluded the local ion flux, i.e. whether the apex represents a depression or protuberance relative to the ion flux direction. Moreover, Sigmund [8] determined that the magnitude of the erosion rate differences was a function of the included angle at the conjunction and the dimensions over which such surface perturbations were important were when they were of the same order as linear dimensions of the energy deposition profile.

As a result of these considerations, Sigmund [8] suggested that some of the conical or pyramidal features frequently observed on eroded surfaces (i) should possess apical angles smaller than those predicted by models which assume a dependence

0022–2461/81/082091–12$03.20/0

of erosion rate only upon the incidence angle of the ion flux, and (ii) show a temporal stability against eradication not predicted by such models. It was also suggested that furrows or trench depressions should form in the pedal region of an inclined boundary at its intersection with a plane normal to the ion flux (e.g. a conical feature contained in a local zone or pit depressed below the extensive surrounding plane area). There is some experimental evidence for both proposals [1, 2, 11–14] but alternative mechanisms for the production of such features based upon local variations in incidence particle flux resulting from ion reflection and sputtered atom redeposition processes have also been advanced [11–15].

Another interesting and frequent experimental observation [1, 2, 20] is that the ion erosion induced the production of regular wave-like facet structures on plane surfaces of crystals, on inclined boundaries between neighbouring polycrystals, on inclined bounding planes of etch pits in crystals and even on the boundary plane of steps produced by differential erosion of amorphized semiconductors possessing a localized protective layer of lower erosion rate material on the initial surface [21]. Such repetitive features have been associated with the generation of regular dislocation networks in the substrate [6, 7], with irradiation enhanced or thermal surface atomic diffusion [22, 23] or with the attempt of the erosion process to relax the surface towards an effective minimum erosion yield condition [22]. The wavelength of such repetitive features often turns out to be of the order of five to ten times the most probable depth of energy deposition below the surface and is thus of the order of the overall cascade dimensions. It is, therefore, possible that some features of this type may depend, for their origin and stabilization, upon the microscopic details and the surface spatial distribution of erosion rate.

In view of these several experimental observations of surface feature development with dimensions comparable to those of average collision cascades, it was felt worthwhile to explore further the effects of local surface morphology in addition to local surface orientation upon local erosion rates. In the present communication we present an approximate analysis of the effects of the immediate environment on the erosion rate at an isolated surface point, illustrating the importance of local curvature, and outline how a more distant environment may be treated in a higher order approximation. It is then shown how the spatial–temporal development of surfaces may be predicted assuming a product function for erosion rate (or sputtering yield) which combines the effects of both surface orientation and local curvature. In this analysis it is shown how a simple erosion slowness theory [3–5] for orientation-dependent erosion rate only is easily modified to include curvature-dependent erosion in a similar manner to that of spatially variable incident flux erosion slowness theory [18]. Finally, some predictions of time-dependent and steady-state morphological forms are examined. Such predictions will be approximate and intuitive since, as will be demonstrated in Section 2, the curvature dependence and distant environment influence upon erosion can only be guessed.

2. Influence of local surface morphology on sputtering yield

Although many experimental studies of the variation of sputtering yield, $Y(\theta)$, for various ion–solid systems as a fuction of incidence angle (θ) between ion flux and surface normal, have been conducted, they refer to measurements from either flat planar surfaces or to surfaces of which the radius of curvature is much larger than the dimensions of individual or average recoil collision cascades. It is well known that the $Y(\theta)$ functuion, for random solids, increases from a minimum at $\theta = 0$, to a maximum at $\theta = \theta_p$ and declines towards zero as $\theta \to \pi/2$. The behaviour of $Y(\theta)$ for small θ can be modelled satisfactorily [24] but for $\theta \gtrsim \theta_p$ theory is inadequate. A major problem in modelling $Y(\theta)$ for large θ is the incomplete development of the collision cascade beneath the solid surface, a problem which will also assume importance in the subsequent examination of curvature-dependent sputtering. Since no experimental data, or theoretical models, are available for the sputtering yields of curved surfaces we shall attempt here a simplified analysis based upon similar arguments to those advanced by Sigmund [8].

For simplicity we consider, as shown in Fig. 1, the differential sputtering yield of an infinitesimal arc length $\delta s'$ in the vicinity of a point $B(x', y')$ on a two-dimensional surface generator $S(x, y)$ in the $x\,0\,y$ plane, resulting from impact of J ions $\sec^{-1}$ per unit length of the surface in the vicinity of a point $A(x, y)$. Following Sigmund [8], the differential sputtering yield at B may be written

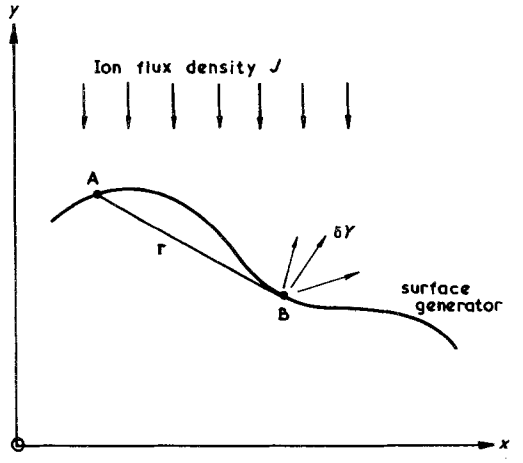

Figure 1 Schematic representation of sputtering at point B(x', y') on surface generator resulting from ion impact at point A(x, y) distant r from A.

$$\delta Y(x', y', x, y) = Jk_1 F_D(\mathbf{r}) \cdot \delta s \, \delta s', \qquad (1)$$

where δs and $\delta s'$ are infinitesimal arc lengths at A and B measured along the surface, $F_D(\mathbf{r})$ is the energy deposition density at B_1 vector distance r, from the point of ion impact at A, and k_1 is a constant dependent upon ion mass and energy and substrate mass and energy of atomic sublimation.

In a full treatment of the effects of total environment on the local sputtering yield at B it would be necessary to integrate Equation 1 over all s, inserting an assumed form for $F_D(\mathbf{r})$ and where $\mathbf{r}^2 = (x' - x)^2 + (y' - y)^2$ would be determined from a prescribed instantaneous form for the surface profile $S(x, y)$.

Sigmund [8] presented such an analysis for (1) semi-infinite intersecting line (or plane) functions for $S(x, y)$, and (2) a Gaussian approximation to $F_D(\mathbf{r})$ [25]. As indicated earlier, the present studies will concentrate upon local rather than distant environment and so the full behaviour of $S(x, y)$ will be ignored. In addition, whereas Sigmund [8] adopted the more correct [25] elliptical symmetry approximation to $F_D(\mathbf{r})$, for analytical convenience a circular approximation will be employed here.

The simplified approach is now depicted in Fig. 2. A uniform flux density J ions $\sec^{-1}$ per unit length of surface is assumed to impinge normally in the $-0y$ direction on to a line surface which is everywhere parallel to $0x$ except for a small depressed region. This region is of length $2l$ projected on to $0x$, of the radius of curvature R, counted positively here for a concave depression, and of included angle $2\theta_m$ at the centre of curvature.

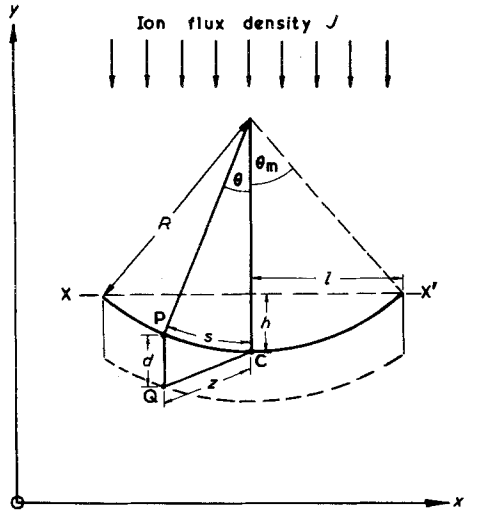

Figure 2 The geometry employed to deduce the sputtering yield Y resulting from ions impacting uniformly (density J) over an arc of surface of radius R.

Each ion is assumed to generate a collision cascade, and thus result in a spatial distribution of energy deposition, centred on a depth d below the point of ion impact on the surface. As a simplifying approximation, the energy deposition function is then assumed to be

$$F_D(\mathbf{r}) = \frac{k_2}{d^2} \exp\left(-\frac{\mathbf{r}^2}{d^2}\right). \qquad (2)$$

In comparison with the more correct elliptical approximation [8] to the energy deposition function, Equation 2 identifies d with the mean depth of energy deposition and the standard deviations in the x and y directions of the energy deposition function.

Considering ions impacting near point P on the surface within the arc XX', the differential sputtering yield at the centre C of the arc, per unit length of arc at C, is given by

$$\delta Y_c = k_1 J \cdot \delta s \cos\theta \cdot \frac{k_2}{d^2} e^{-z^2/d^2}, \qquad (3)$$

where Q, the centre of the cascade, is located distance d from P and distance z from C. The factor $\cos\theta$ arises from the projection of the arc length δs measured from C at P upon the $0x$ direction.

From the geometry of Fig. 2 it is readily deduced that, for small θ,

$$QC^2 \approx PQ^2 + QC^2 - 2PQ \cdot QC \cos Q\hat{P}C$$

or

$$z^2 \approx d^2 + R^2\theta^2 = 2dR\theta \sin\theta \qquad (4a)$$

since

$$\mathrm{PC} = s \approx R\theta. \qquad (4b)$$

Thus, in small-angle approximation,

$$z^2 = d^2 + R^2\theta^2 - 2dR\theta^2 \qquad (4c)$$

or

$$z^2 = d^2 + \theta^2(R^2 - 2dR). \qquad (4d)$$

To obtain the total sputtering yield at C it is necessary to integrate Equation 3 over three regions, i.e. from $-\infty$ to X, from X to X′ and from X′ to $+\infty$. In view of the exponentially decaying nature of the energy deposition function of Equation 2, however, the major contributions to sputtering at C will be from ion impact on surface points P close to C such that z is of order d and thus Equation 3 may be integrated only over the region $-\theta_m \leqslant \theta \leqslant +\theta_m$. Thus

$$Y_c \cong \frac{k_1 k_2}{d^2} J \cdot R \times \int_{-\theta_m}^{\theta_m} \mathrm{d}\theta \exp\left[-\left\{1 + \theta^2\left(\frac{R^2}{d^2} - \frac{2R}{d}\right)\right\}\right]. \qquad (5)$$

Provided that $\theta^2[(R^2/d^2) - (2R/d)]$ is small, the exponential term may be expanded to first order and integrated to give

$$Y_c \cong \frac{k_1 k_2}{d^2} J \cdot R\, \mathrm{e}^{-1} \times \left[2\theta_m - \frac{2\theta_m^3}{3}\left(\frac{R^2}{d^2} - \frac{2R}{d}\right)\right] \qquad (6)$$

for small θ_m, $\theta_m \approx l/R$. Thus

$$Y_c \approx 2\frac{k_1 k_2}{d^2} Jl\, \mathrm{e}^{-1} \times \left|1 - \frac{1}{3}\frac{l^2}{R^2}\left(\frac{R^2}{d^2} - \frac{2R}{d}\right)\right|. \qquad (7a)$$

As $R \to \infty$, i.e. the flat plane condition,

$$Y_c(\infty) \to \frac{2k_1 k_2}{d^2} J \cdot l \cdot \mathrm{e}^{-1}\left(1 - \frac{l^2}{3d^2}\right) \qquad (7b)$$

and thus the yield ratio for curved to flat surfaces is given by

$$\frac{Y_c(R)}{Y_c(\infty)} \approx 1 + \frac{\frac{2}{3}(l^2/Rd)}{1 - \frac{1}{3}(l^2/d^2)}. \qquad (7c)$$

Since

$$\frac{l^2}{d^2} \approx \frac{R^2\theta_m^2}{d^2}$$

has been assumed small, then

$$\frac{Y_c(R)}{Y_c(\infty)} \approx 1 + \frac{2l^2}{3Rd}. \qquad (7d)$$

Equation 7b reveals the expected result that, as the depth of the centre of the collision cascade (d), increases, so the sputtering yield decreases. Equation 7d, however, reveals that the curved surface yield may be enhanced or reduced relative to the plane surface yield depending upon the sign and magnitude of the radius of curvature R, the length of arc (approximately l) of the curved region and the magnitude of the depth of the centre of the collision cascade d ($d > 0$ always).

It may be noted that similar conclusions as to the influence of R, l and d may be deduced if the integrated yield over the whole arc is determined rather than the value only at its centre. It may also be noted from Equation 7d that for positive radius of curvature (a depression), the sputtering yield of the curved surface is greater than that of a flat surface whereas for a negative radius of curvature (a protuberance) the sputtering yield of the curved surface is lower than that of a flat surface. The enhancement or eduction increases in importance as R decreases. Thus for surface feature dimensions of the order of the collision cascade dimensions the variation of sputtering yield predicted above corresponds in sense to the analysis of Sigmund [8] of the enhanced yield at the depressed intersection of semi-infinite planes and the reduced yield of a protuberant intersection.

The preceding equations were derived assuming average normal incidence (i.e. θ_m small) of the ion flux J to the arc and the surrounding plane. If the flux is inclined to an arc surface, but the included angle $2\theta_m$ is small, then an approximate idea of the behaviour of the yield may be obtained by replacing the depth of the cascade centre (d) by the $0y$ projection, $d\cos\theta$. The flat plane yield will thus vary as $\sec^2\theta$, from Equation 7b whereas, of course, the full plane surface integration leads to an approximate $\sec^{5/3}\theta$ dependence [24] for $\theta < \theta_p$. The $d\sec\theta$ projection will also moderate the bracketted term in Equation 7d and thus the curved surface:plane surface sputtering yield ratio will also depend upon the macroscopic angle of ion flux impingement through the R, l and d dependent term.

Since current theory does not adequately predict the $Y(\theta)$ function for plane surfaces for $\theta \gtrsim \theta_p$, the present theory (which owes similar origins to the plane surface theory) cannot be anticipated to reasonably predict the $Y(\theta)$ dependence for curved surfaces either. The major problem of the flat plane theory, as clearly stated by Sigmund [8], is that, as the macroscopic angle θ increases, the collision cascade will be incompletely developed beneath the solid surface and thus $Y(\theta)$ falls for $\theta \gtrsim \theta_p$. In the present context, this problem is even more serious when the surface is considered curved and the radius of curvature and arc dimensions are of order of the collision cascade dimensions d. Under these circumstances, which are essentially those discussed in the above simplified model, the detailed dependence for $Y(R)$ deduced earlier, cannot be expected to *accurately* represent the R, l, d and θ dependences of the curved surface yield. Nevertheless, and as argued by Sigmund [8], the types of relationship derived in Equations 7 indicate *some* form of dependence of local sputtering yield upon local radius of curvature, local dimensions and cascade dimensions, when the macroscopic surface parameters R and l are of order d. There is also a variable influence of macroscopic incidence angle θ upon the extent of the moderation of sputtering yield due to surface curvature. On the basis of Equation 7d, therefore, we may write, as a first approximation,

$$Y(\theta \cdot R) = Y(\theta, \infty) g(\theta, R, l, d), \qquad (8)$$

i.e. the sputtering yield of a curved surface is equal to that of the plane surface at the same mean angle of ion flux incidence moderated by some unknown function of the local surface dimensional and angular parameters. Since the preceding analysis is so approximate, we prefer not to hazard even a guess at the form of the function g, but note that is will assume importance when macroscopic surface dimensions are of the order of cascade dimensions. Even this inexact conclusion will allow further progress on a generalized study of surface morphological evolution, however, as shown in the next section.

3. Second-order erosion slowness theory

When the sputtering yield $Y(\theta)$ is a function of θ only, the deduction of the time evolution of an initially contoured surface is a relatively straightforward process and may be accomplished graphically or computationally, but not generally analytically, because of the complex nature of the defining equations. The nature of these equations, however, does give clear guidance as to the calculation schemes to be followed and the rules to be obeyed.

In an earlier analysis of surface topographic evolution, Carter *et al.* [3, 5] showed that if the space–time motion of points on a surface of orientation θ to the ion flux was followed, then for uniform flux density J, the defining equations for θ were

$$\left.\frac{\partial \theta}{\partial t}\right|_x = -\frac{J}{n}\frac{\mathrm{d}Y}{\mathrm{d}\theta}\cos^2\theta \cdot \left.\frac{\partial \theta}{\partial x}\right|_t \qquad (9a)$$

and

$$\left.\frac{\partial \theta}{\partial t}\right|_y = \frac{J}{n}\left\{\frac{\mathrm{d}Y}{\mathrm{d}\theta}\sin\theta\cos\theta - Y\right\}\left.\frac{\partial \theta}{\partial y}\right|_t, \qquad (9b)$$

where n is the solid atomic density.

In a complementary analysis, Barber *et al.* [4] showed that the sputtering-induced surface development may be treated on a similar basis to the chemical dissolution of crystals which is itself well described by Frank's [26, 27] application of kinematic wave theory. Carter *et al.* [5] also showed that Equations 9a and 9b were of the kinematic wave type and were essentially hyperbolic equations [28]. Equations 9a and 9b indicate that the spatial components of velocity of surface points maintaining constant orientation θ are

$$v_{x|\theta} = \frac{J}{n}\frac{\mathrm{d}Y}{\mathrm{d}\theta}\cos^2\theta \qquad (10a)$$

and

$$v_{y|\theta} = \frac{J}{n}\left\{\frac{\mathrm{d}Y}{\mathrm{d}\theta}\sin\theta\cos\theta - Y\right\} \qquad (10b)$$

and thus the total vector velocity of points of constant orientation θ is given by

$$\begin{aligned} v_\theta^2 &= v_x|_\theta^2 + v_y|_\theta^2 \\ &= \left(\frac{J}{n}\right)^2\left\{\left(\frac{\mathrm{d}Y}{\mathrm{d}\theta}\cos^2\theta\right)^2 + \left(\frac{\mathrm{d}Y}{\mathrm{d}\theta}\sin\theta\cos\theta - Y\right)^2\right\} \\ &= \left(\frac{J}{n}\right)^2\left\{\left[\frac{\mathrm{d}}{\mathrm{d}\theta}(Y\cos\theta)\right]^2 + (Y\cos\theta)^2\right\}. \qquad (10c) \end{aligned}$$

The direction of motion of such points of constant orientation θ is given by

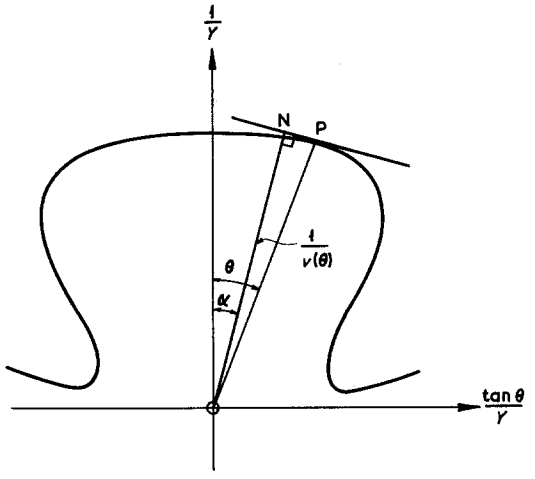

Figure 3 Erosion slowness plot ($1/Y\cos\theta$ as a polar function of θ) illustrating the deduction of the characteristic velocity ($v(\theta)$) and direction (α) of a surface element maintaining a constant orientation θ during erosion.

$$\tan\alpha = \frac{\dfrac{dY}{d\theta}\sin\theta\cos\theta - Y}{\dfrac{dY}{d\theta}\cos^2\theta}. \qquad (10d)$$

Carter *et al.* [5] showed that these velocity parameters could be represented on the erosion slowness plot developed by Barber *et al.* [4] where the reciprocal surface normal erosion rate $OP = n/JY\cos\theta$ of a point of orientation θ is plotted as a function of θ, by the reciprocal magnitude and the direction of the normal 0N from the origin of the erosion slowness plot to its intersection with the tangent to the erosion slowness plot at the surface orientation θ. Equations 10c and 10d also illustrate that the spatial direction and velocity of motion of points maintaining constant orientation θ as the surface changes in time are constants and thus the loci of points of constant orientation θ are straight lines. These properties of the erosion slowness plot are illustrated in Fig. 3. Barber *et al.* [4] also showed that if two neighbouring points of orientation θ_1 and θ_2 on the surface followed intersecting trajectories, then at the point of intersection an edge developed (i.e. a zero radius discontinuity on the surface). The velocity and direction of the motion of this edge were then determined from the erosion slowness plot from the normal from the origin to the chord joining the points of orientation θ_1 and θ_2 on the erosion slowness plot. Such edges were identified by Carter *et al.* [3, 5] as equivalent to the motion of intersecting linear surface segments developed in an earlier theory of topography development by Stewart and Thompson [29]. It was also shown [3, 5] that the loci of such edges were not necessarily linear.

The application of these concepts to the study of the evolution of surface morphology has been undertaken by Barber *et al.* [4], Carter *et al.* [5], Ducommun *et al.* [30, 31] and Witcombe [32]. The major conclusions which may be reached for a random isotropic solid are that (1) the final, steady-state morphology developed from an initially randomly undulating surface is a flat plane (or segments of parallel flat planes) of that orientation contained within the full range of orientations of the initial profile, relative to the ion flux, which represents a minimum erosion rate parallel to the ion flux; (2) only orientations initially present (or potentially present via inclusion within the range of initial orientations) will exist at any stage of erosion; (3) during dynamic evolution pyramidal, ridge and boundary protuberant structures inclined at an angle θ_p to the ion flux may form transiently but be later eroded. The flat plane form results from the requirement that the characteristic trajectories must all be parallel on the erosion slowness plot and that the vector velocity v_θ be minimized. Another useful result of this first-order theory is that the rate of change of radius of curvature of a surface element maintaining constant orientation θ may also be deduced to be [5, 9, 31]

$$\left.\frac{\partial R}{\partial t}\right|_\theta = \frac{J}{n}\left\{\frac{d^2Y}{d\theta^2}\cos\theta - 2\frac{dY}{d\theta}\sin\theta\right\}. \qquad (11)$$

Recently Carter *et al.* [16], Smith and Walls [17, 19] and Nobes *et al.* [18] have further extended the above form of erosion slowness theory to include the more general case of spatially variable ion flux density $J(x, y)$. It was shown [16, 18] that in this case, Equations 10a and 10b become

$$\left.v_x\right|_\theta = \frac{1}{n}\frac{d(JY)}{d\theta}\cos^2\theta \qquad (12a)$$

and

$$\left.v_y\right|_\theta = \frac{1}{n}\left\{\frac{d(JY)}{d\theta}\sin\theta\cos\theta - JY\right\}. \qquad (12b)$$

However it was also deduced that it was more valuable to consider the motion of points on the time-developing surface, which maintained not constant orientation θ but constant value of the product $J \cdot Y$. For spatially uniform J this corre-

sponds to a constant Y and concomitantly constant orientation θ. In the constant JY framework it was shown that corresponding results to Equation 12 may be deduced as

$$v_x\Big|_{JY} = \frac{J}{n}\frac{\mathrm{d}Y}{\mathrm{d}\theta}\cos^2\theta \tag{13a}$$

and

$$v_y\Big|_{JY} = \frac{J}{n}\cdot\left\{\frac{\mathrm{d}Y}{\mathrm{d}\theta}\sin\theta\cos\theta - Y\right\}. \tag{13b}$$

The importance of these results is that for constant JY the vector velocity $v|_{JY}$ is identical to that given by Equation 10c for constant orientation θ provided that the spatially appropriate value of J is chosen and that the direction $\tan\alpha|_{JY}$ is identical to that given by Equation 10d independent of J.

This means that the erosion slowness curve depicted in Fig. 3 for spatially uniform flux density J can be used equally readily for spatially non-uniform J as follows. For all known values of J over the real surface, erosion slowness curves are constructed similar to the one shown in Fig. 3, and which are merely magnitude scaled in J but unchanged in θ dependence. Points on the initial surface of known J and Y (hence θ) are chosen and the appropriate erosion slowness plots for each value of J are consulted to give the magnitude and direction of motion of each surface point. The motion of each surface point is then determined for a fixed time step δt (or local ion density step $J\delta t$) and a new surface reconstructed from the individual point motion. This step carries each surface point into a changed J value so that the next iteration proceeds with modified J and θ for each surface point and the appropriate erosion slowness plots for each J value must be again consulted. This process is continued to study the dynamic development of the surface morphology. It turns out [16], just as in the constant Jcase, that edges may form with transient form and produce quasi-conical protuberances and depressions but except under very specific conditions of the $Y(\theta)$ form and the $J(x, y)$ variation, no steady-state end forms can result, i.e. the surface morphology is constantly changing.

In spatially uniform flux density conditions, the characteristic trajectories or loci of points of constant orientation are straight lines, whereas in spatially variable flux density conditions, the orientations of surface points for which the product JY is constant are constantly changing. Indeed it is readily shown that the variation of θ along a constant JY trajectory is described by [18, 19]

$$\frac{\partial\theta}{\partial t}\Big|_{JY} = -\frac{Y\cos^2\theta}{n}\frac{\partial J}{\partial x}\Big|_{JY}. \tag{14}$$

This equation provides an alternative means of following the dynamic development of an eroded surface since, if the initial surface is prescribed and values of θ are known and if the spatial variation of J is prescribed, then the change $\delta\theta$ in orientation θ and the changed co-ordinates of the point may be deduced since the generated erosion slowness plot describes the magnitude and direction of motion uniquely for all θ. For short time steps, J may be assumed constant.

As in the spatially uniform J case, edges must be handled specially and the motion of edges is determined from chord construction *between* erosion slowness plots of different J_1 and J_2 flux densities appropriate to the neighbouring points of orientations θ_1 and θ_2. It should also be emphasized that, whereas in the constant J case, only orientations present in the initial surface can be maintained [26] new orientations may emerge in the variable J condition (Equation 14).

The reason for the preceding review of current erosion slowness theory is that it provides an important starting point for evaluating surface morphological change when the erosion rate is not merely a function of ion flux density and incidence angle but may also be a function of local environment.

Considering, for simplicity, the case of constant ion flux density then, if the product function of Equation 8 can be assumed to represent the effects of incidence angle and local environment on the sputtering yield of curved surfaces at mean inclination θ, the surface normal erosion rate ρ_n may be written

$$\rho_n = -\frac{J}{n}Y(\theta)\cdot\cos\theta\cdot g. \tag{15}$$

Use of this expression then leads to equations for $v_x|_\theta$, $v_y|_\theta$, v_θ, $\tan\alpha|_\theta(\partial R/\partial t)|_\theta$ identical to those of Equations 10 to 13 except that JY is everywhere replaced by $JY\cdot g$. This result arises since Equation 9a for example, derives from the equation

$$\frac{\partial\theta}{\partial t}\Big|_x = \cos^2\theta\,\frac{\partial}{\partial\theta}(\rho_n\sec\theta)\frac{\partial\theta}{\partial x}\Big|_t \tag{16}$$

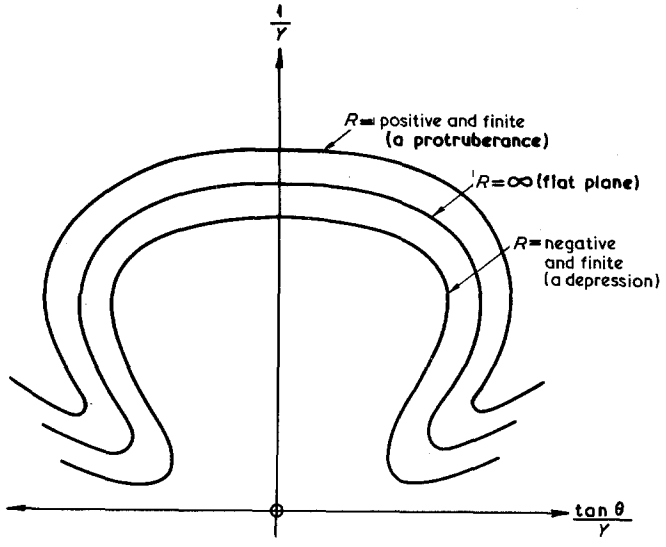

Figure 4 A hypothetical family of erosion slowness plots where the $g(R)$, radius of curvature moderating function on $Y(\theta)$ is independent of orientation θ.

or

$$\left.\frac{\partial\theta}{\partial t}\right|_x = h(\theta, x, t)\left.\frac{\partial\theta}{\partial x}\right|_t,$$

where $h(\theta, x, t)$ is some function of θ, x and t.

Equations of this type can generally be analysed in terms of the characteristics method applicable to hyperbolic equations [28]. The erosion slowness technique is a special case of the characteristics approach. Indeed, even if more distant effects than the local effects considered here, when integrated over all space, lead to a defining equation for the local variation of θ, of the form of Equation 16, the characteristics method can be used, in principle, to evaluate the surface morphology development.

Essentially this means that in the present approximation where the generalized sputtering yield at orientation θ, is written as a product function of the corresponding yield for the flat surface condition ($Y(\theta, \infty)$) and a function describing local environment influence (which may itself be a function of θ), all equations which describe the flat plane erosion case with given $Y(\theta, \infty)$ also describe the curved surface development provided that $Y(\theta, \infty)$ is everywhere moderated by the g function appropriate to local conditions. The importance of this recognition is that, just as in the variable ion flux density case where J moderates Y locally, so does g moderate Y locally and thus we can again construct a family of erosion slowness curves for each g function. Consequently, if the $Y(\theta, \infty)$ function for the flat plane condition is known, this provides the basic erosion slowness curve and for each value of $1/[Y(\theta, \infty)\cos\theta]$ on this curve we can construct a variation about this value by multiplication by an appropriate g^{-1} function at each θ value. Although straightforward in principle, the discussion of Section 2 illustrates the practical difficulties of deducing a g function appropriate to all local environment and orientation conditions. In general, however, it might be expected that the effect of the g function would be to broaden the single $Y(\theta, \infty)$ function into some band function. A hypothetical example is given in Fig. 4 where it is assumed that g increases with decreasing radius of curvature R to some limiting values (defining the band limits of the erosion slowness family of curves), such that $g > 1$ for $R > 0$ (i.e. a depression) and $g < 1$ for $R < 0$ (i.e. a protuberance) and g is independent of θ. Once the form of g is specified (known or assumed) the erosion slowness concepts outlined earlier may be readily applied to deduce the time-dependent surface morphological development of an initially prescribed surface. Thus it is possible to follow either the progress of surface points maintaining constant $Y(\theta)\cdot g$ in space by employing Fig. 4 for the appropriate erosion velocities (and directions) at each g value on the initial and developing curves *or* in the special case where g is independent of θ (as in Fig. 4), the progress of surface points maintaining constant orientation θ. In this case the g function represents an orientation independent moderation of the velocity and direction of motion of such points as shown by Equations 12a and 12b for $g(\theta)$ independent of θ. Even in the case where g is not independent of orientation θ, the generalized family of erosion

slowness curves may still be employed to monitor the evolution of a surface profile since each point on the initial surface can be assigned θ (and hence $Y(\theta)$) and local environment (hence g) values so that there will be corresponding velocities and directions of motion for each point somewhere on the erosion slowness family. The co-ordinates of surface point may then be incrementally adjusted over a time step and new co-ordinates deduced, thus moving each surface point on to a different erosion slowness curve. The process is iterated to determine the temporal development of the surface. When local erosion rate is not a simple product function of the flat plane yield and local feature habit, or when more distant effects are to be included, then erosion slowness curves will be of limited value, but once the local erosion rate ρ_n can be prescribed, the use of characteristic methods [28] is still available. Moreover, if local accretion processes, resulting from, for example, surface and volume diffusion [9, 10], condensation of sputtered atoms [15] etc., are operative, then, provided that the nett local erosion rate ρ can be derived as a definable difference in erosion rate ρ_n and accretion rate ρ_a, all of the preceding discussion is applicable with ρ replacing ρ_n everywhere (e.g. in Equation 16). Consequently, erosion slowness and/or characteristics methods are generally applicable in circumstances of erosion and/or growth.

When erosion rate is a function of local environment there are two important questions to be answered. Firstly, how may the time-dependent surface morphology and secondly, how may the time-independent surface morphology (i.e. any steady-state morphology) differ from those when erosion rate is local environment independent? The second of these questions is somewhat easier to answer from consideration of the erosion slowness concepts. Thus steady state is only achieved, i.e. a surface maintains a time-independent form, when the velocities and directions of motion of points of all constant orientations in the surface are equal. The velocity and direction of motion of a point on a surface is given by the inverse magnitude and direction of the normal from the origin to the tangent to the erosion slowness curve at the orientation of the surface point and appropriate to the local environment of that point. Consequently, if a range of orientations and local environments is to form the steady-state profile, the locus of points of constant $(v(\theta)g)^{-1}$ on the family of erosion slowness curves must be a straight line. Moreover, the tangents to each of the erosion slowness profiles at these constant $(v(\theta)g)^{-1}$ points must be parallel. In this way *only* are the normals for neighbouring g function erosion slowness curves equivalent in magnitude and direction. For the orientation-independent g function family of erosion slowness curves, illustrated in Fig. 4, this condition cannot be fulfilled for any θ (or range of θ). Thus any steady-state morphology for a θ-independent g function must possess a single value of θ. According to the concepts developed in g-independent erosion slowness theory, the most stable [4, 5, 33] steady-state morphology, of constant orientation θ is achieved for minimum v_θ in the available range of θ orientations present on the initial surface since other erosion trajectories finally merge and collapse into this state. This trajectory intersection process will also occur for local environment-dependent erosion so that the most stable orientations will correspond to v_θ minimization. In erosion slowness curves of the form shown in Figs 3 and 4 this generally corresponds to $\theta = 0$, i.e. the erosion flux normal to the surface. The smallest minimum in v_θ, when erosion is g dependent also, will then denote the most stable surface configuration. In the context of Fig. 4 this suggests a final surface morphology of small hemispherical protuberant caps of radii and heights which minimize local erosion and preserve a close approximation to $\theta = 0$. In this case, hemispherical depressions would be excluded from the steady-state morphology since they represent enhanced values of g relative to the flat plane or convex surface and are thus typical of larger values of v_θ than are these latter configurations.

It is not impossible to conceive, however, that a more subtle form of $g(\theta)$ may operate such that for both positive and negative radii of curvature, minima in the $Y(\theta) \cdot g(\theta)$ function may occur over an extended angular interval near $\theta = 0$. If such is the case then a steady-state morphology consisting of bumps and depressions of varying radii of curvature could result. Such forms have been inferred from scanning electron microscopic studies of normal incidence ion-bombarded Ge by Wilson [34]. However, although a hypothetical $Y(\theta) \cdot g(\theta)$ function may be postulated, which gives rise to an extended minimum, it should be considered unlikely. In particular, as pointed out by Sigmund [8] and confirmed here in the earlier discussion,

protuberances of cascade dimensions should possess lower sputtering yields than both macroscopic protuberances of similar orientation and flat planes of $\theta = 0$ orientation, whereas the opposite is true for cascade-sized depressions. Thus a combination of small-angled cones contained within a pedal depression surrounded by a flat plane would *not* be a stable end form.

It should be noted, therefore, that if there is no local environment (radius of curvature) dependence of the sputtering yield near the local minimum at $\theta = 0$, but a marked dependence for larger θ (e.g. in the region of $\theta = \theta_p$) then the steady-state morphology will be a flat plane or segments of planes and not some morphology relating to an undulatory surface composed of components with radii of curvature corresponding to minimum (peaks) and maximum (troughs) rates of erosion. Thus the generation of ripple forms resulting from the sandblasting erosion of ductile solids, in which the general theory of erosion was shown by Carter *et al.* [35] to be identical to that of the erosion slowness formalism developed above, cannot result from the radius of curvature and incidence angle variations of erosion rate alone, as suggested by Finnie and Kabil [36]. It should be noted, however, that the suggestion that erosion processes may possess both orientation and curvature dependence was first indicated by Finnie and Kabil [36] and although these authors did not recognize the utility of erosion slowness methods they did deduce, correctly, the motion of surface points given by Equation 15.

Although steady-state conditions did not result from a combination of minimum and maximum erosion conditions, intermediate conditions may contain such forms as is the case for g-independent erosion where transient peak and valley structures may occur. We therefore turn attention to the dynamic development of the morphology.

Rather than selecting a variaty of specific initial surface contours (e.g. sphere [4], sine wave [31, 37, 38], etc.) or a well-determined form for the g function, we will make some general observations arising from the earlier discussion which will be applicable in all situations. We may note from Equation 11 (with gY substituted for Y), Equations 12, 13 and 14, that if the initial surface contour θ is everywhere constant so that g is independent of θ there is (1) no variation of the rate of change of radius of curvature with initial surface co-ordinates for fixed orientation, (2) all surface orientations follow identical characteristic trajectories (e.g. v_θ, v_{xy}, and $\tan\alpha$ are invariant on the initial surface), and (3) there is no change in orientation along constant gY trajectories. This implies that for a perfectly flat initial surface no erosional shape change will occur, and that an infinite plane initially inclined at any arbitrary angle θ_a to the ion flux will maintain that geometry for all erosion time. This is a different result [16] from the case of spatially variable ion flux J where, *ab initio*, J is a function of space co-ordinates so that $\mathrm{d}J/\mathrm{d}x$ is finite whereas initially (and thus for all time) $\mathrm{d}g/\mathrm{d}x$ is zero. The important conclusion is, therefore, that *only* if the initial surface is perturbed from the planar condition can time-variable morphology occur. Even with the best prepared surfaces, one would expect some initial surface non-uniformity on the atomic and large scales whilst the existence of extended defects (e.g. dislocations and inclusions such as surface and bulk impurities precipitates) could perturb the local sputtering yield Y. In addition, the ion bombardment itself may generate [1, 2] further imperfections such as dislocations and gas bubbles whilst fluctuations in local sputtering yield may give rise to craters of multi-atomic dimensions [39, 40]. In such cases, local departure from planity can result and the potential for non-uniform erosion be realized. The subsequent development of such perturbations will then depend intimately on the real initial surface contour and upon the actual g function. However, and as in the case of g-independent erosion, Equation 11 reveals that for each initial orientation θ, the sign and magnitude of the time rate of change of curvature of a surface element depends upon the difference between $[\mathrm{d}^2(gY)/\mathrm{d}\theta^2]\cos\theta$ and $[2\mathrm{d}(gY)/\mathrm{d}\theta]\sin\theta$. Thus, potentially, protuberant and depressed structures with small radii of curvature may enlarge or contract depending upon the local behaviour of these two functions. Moreover, Equation 14 indicates that new orientations, not initially present in the surface contour, may also develop except in the unique case of an initially flat plane. It is thus expected that features of dimensions initially less than cascade dimensions could initially enlarge relative to their surroundings since their erosion trajectory parameters (v and α) could differ from those of the surroundings. This conclusion concurs with that of Sigmund [8] regarding the potential development of subcascade dimensional features. However, even

if such small features do enlarge or, on the other hand, larger features contract, until some minimum or maximum erosion yield features predominate with dimensions of the order of cascade dimensions, it must be stressed again that these can only be in equilibrium if all of the characteristic trajectories for all surface points are parallel and the erosion velocities equal. Thus, as already noted, whilst temporary protuberant and depressed structures may occur during erosion, as is the case for example in cone formation on a flat surface determined solely by $Y(\theta)$ considerations independent of g moderation, it is quite unlikely that these can represent stable end forms since the probability of congruent $(v(\theta)g)^{-1}$ behaviour for a broad range of orientations must be expected to be low. Thus a morphology of fine tipped or radiused cones surmounting larger angled cones, themselves located within pedal pits in a flat land, is unlikely to represent a stable configuration. However, they may represent a transient stage following the initial formation of a large cone or pyramid on a flat surface resulting either from contaminant protection [1, 2, 12, 29] or otherwise locally perturbed erosion [1, 2] and thus the observations [12, 41, 42] of macroscopic cones developing fine tips during their erosion towards disappearance may arise from the above and similar arguments by Sigmund [8].

The pedal depressions [1, 2, 11–13] surrounding cones may also *initiate* and develop following similar processes but when both cones and depressions become much larger than cascade dimensions it would be expected that the subsequent evolution of the depressions would be more influenced by macroscopic enhancements of local sputtering flux density arising from reflection and directed sputtering processes from protuberances [11–13]. It is also possible that where re-entrant features or jogs develop in the faces of grain boundaries or with etch pits [1, 2, 20] during their preferential erosion that local sputtering yield becomes enhanced (i.e. somewhat equivalent to a depression on a flat surface) thus allowing for the excision of a pyramid structure on such boundaries [1, 2, 20] or the generation of a repetitive facet [1, 2, 20, 43] structure with repetition distance of the order of cascade dimensions. Other potential explanations [22] for such behaviour may be associated with preferential dislocation generation, implanted gas occlusion and ion-bombardment enhanced surface atomic migration but, again, the initiation, if not the temporal relative stability of such features, may be associated with the local perturbational effects discussed here.

In order to be more definitive about the role of such processes, substantially more experimental observations of the dynamic evolution of surface features during bombardment are required, particularly with high magnification and resolution techniques to allow study on the scale of the dimensions of collision cascade. At present, observations refer to a surface status which is generally on a much larger scale than such dimensions. Dynamic observations should allow determination of g functions if conducted over sufficiently small ion fluence (and thus surface morphology change) increments and then allow comparison of further predicted morpholpgical development with theoretical arguments.

4. Conclusions

Following Sigmund's [8] proposal that the sputtering yield of non-planar surfaces may be locally modified where feature dimensions are of similar magnitude to collision cascade dimensions, an attempt has been made here to develop a generalized model to describe the temporal modification of ion-bombarded surfaces which accommodates these local influences. It has been shown that if an appropriate describing function for local effects can be determined (a very approximate form was outlined in Section 2) and if this describing function is merely a multiplier to the conventional surface orientation–sputtering yield function then a slightly modified and generalized form of erosion slowness theory and methods can be developed. This theory has been employed to show that although local environment effects on sputtering yield may lead to the generation of transient structures of dimensions similar to cascade dimensions it is very unlikely that such features can represent time-independent stable end forms. It is suggested that high-resolution experimental studies would be benificial in evaluating the importance of local environment effects and hence in determining the validity of the proposed theoretical approach.

References

1. J. L. WHITTON and G. CARTER, Proceedings of the Symposium on Sputtering, edited by P. Varga, G. Betz and F. P. Viehbock. (Institüt für Allegemeine Physik, University of Wien, 1980) p. 552.

2. G. CARTER, J. L. WHITTON and B. NAVINSEK, in "Sputtering by Ion Bombardment", edited by R. Behrisch (Springer Verlag, Berlin, Heidelberg and New York), to be published.
3. G. CARTER, J. S. COLLIGON and M. J. NOBES, *J. Mater. Sci.* 8 (1973) 1473.
4. D. J. BARBER, F. C. FRANK, M. MOSS, J. W. STEEDS and I. S. T. T'SONG, *ibid.* 8 (1973) 1030.
5. G. CARTER, J. S. COLLIGON and M. J. NOBES, *Rad. Effects* **31** (1977) 65.
6. N. HERMANNE, *ibid.* **19** (1973) 161.
7. R. S. NELSON and D. F. MAZEY, "Ion Surface Interaction, Sputtering and Related Phenomena" (Gordon and Breach, London, (1973) p. 119.
8. P. SIGMUND, *J. Mater. Sci.* 8 (1973) 1545.
9. G. CARTER, *ibid.* **11** (1976) 1091.
10. G. CARTER, J. S. COLLIGON and M. J. NOBES, Proceedings of the 8th Yugoslav Symposium on the Physics of Ionized Gasses, edited by B. Navinsek (Universität Ljubljana, 1976) p. 329.
11. I. H. WILSON and M. W. KIDD, *J. Mater. Sci.* 6 (1971) 1632.
12. I. H. WILSON, *Rad. Effects* **18** (1973) 95.
13. A. R. BAYLY, *J. Mater. Sci.* 7 (1972) 404.
14. W. HAUFFE, *Phys. Stat. Sol. (a)* **4** (1971) 111; **35** (1976) K93.
15. G. BELSON and I. H. WILSON, Proceedings of the Symposium on Sputtering, edited by P. Varga, G. Betz and F. P. Viehbock (Institüt für Allgemeine Physik, Universität Wien, 1980) p. 574.
16. G. CARTER, M. J. NOBES, K. I. ARSHAK, R. P. WEBB, D. EVENSON, B. D. L. EGHAWARY and J. H. WILLIAMSON, *J. Mater. Sci.* **14** (1979) 728.
17. R. SMITH and J. M. WALLS, *Surface Sci.* **80** (1979) 557.
18. M. J. NOBES, R. P. WEBB, G. CARTER and J. L. WHITTON, *Rad. Effects Letters* **50** (1980) 133.
19. R. SMITH and J. M. WALLS, *Phil. Mag* **A42** (1980) 235.
20. J. L. WHITTON, G. CARTER, M. J. NOBES and J. S. WILLIAMS, *Rad. Effects* **32** (1977) 129.
21. H. DIMIGEN and H. LUTHJE, *Phillips Tech. Rev.* **35** (1975) 199.
22. G. CARTER, M. J. NOBES, G. W. LEWIS and J. L. WHITTON, *Rad. Effects Letters* **50** (1980) 97.
23. L. T. CHADDERTON, *ibid.* **43** (1979) 91.
24. P. SIGMUND, *Phys. Rev.* **184** (1969) 383.
25. K. B. WINTERBON, P. SIGMUND and J. B. SANDERS, *Mat. Fys. Medd. Dan. Vid. Selsk.* **37** (1970).
26. F. C. FRANK, "Growth and Perfection of Crystals" (John Wiley and Sons, New York, 1958) p. 411.
27. *Idem, Z. Phys. Chem. Neue Folge* 77 (1972) 84.
28. G. B. WHITHAM, "Linear and Non Linear Waves" (John Wiley and Sons, New York, 1974).
29. A. D. G. STEWART and M. W. THOMPSON, *J. Mater. Sci.* 4 (1969) 56.
30. J. P. DUCOMMUN, M. CANTAGREL and M. MOULIN, *ibid.* **10** (1975) 53.
31. J. P. DUCOMMUN, M. CANTAGREL and M. MARCHAL, *ibid.* 9 (1974) 725.
32. G. CARTER, M. J. NOBES and J. L. WHITTON, *ibid.* **13** (1978) 2725.
33. M. J. WITCOMB, *ibid.* **10** (1975) 669.
34. I. H. WILSON, Proceedings of the Symposium on Sputtering, edited by P. Varga, G. Betz and F. P. Viehbock, (Institüt für Allgemeine Physik, Universität Wien. 1980) p. 584.
35. G. CARTER, M. J. NOBES and K. I. ARSHAK, *Wear* **53** (1979) 245.
36. I. FINNIE and Y. H. KABIL, *ibid.* 8 (1965) 60.
37. C. CATANA, J. S. COLLIGON and G. CARTER, *J. Mater. Sci.* 7 (1972) 467.
38. T. ISHITANI, M. KATO and R. SHIMIZU, *J. Mater. Sci.* 9 (1974) 505.
39. K. MERKLE, Proceedings of the Symposium on Sputtering, edited by P. Varga, G. Betz and F. P. Viehbock (Institüt für Allgemeine Physik, Universität Wien, 1980) p. 124.
40. D. N. SEIDMAN, M. I. CURRENT, D. PRIMANIK and C.-Y. WEI, Proceedings of the International Conference on Ion Beam Modification of Materials, (Albany, New York, 1981) to be published.
41. G. W. LEWIS, J. L. COLLIGON, F. PATON, M. J. NOBES, G. CARTER and J. L. WHITTON, *Rad. Effects Letters* **43** (1979) 49.
42. O. AUCIELLO, R. KELLY and R. IRICIBAR, *ibid.* **43** (1979) 37.
43. J. J. TRILLAT, "Ionic Bombardment, Theory and Applications" (Gordon and Breach, New York, 1964) p. 13.

Received 27 October 1980 and accepted 8 January 1981.